1st Virtual European Conference on Fracture

Closed-form dispersion relationships in bond-based peridynamics

Bingquan Wang[a,*], Selda Oterkus[a], Erkan Oterkus[a]

aPeriDynamics Research Centre, Department of Naval Architecture, Ocean and Marine Engineering, University of Strathclyde, 100 Montrose Street, Glasgow G4 0LZ, UK

Abstract

Classical continuum mechanics (CCM) has been widely used in structural analysis for the last two centuries. Dispersion curves, which describes the relationship between wave frequency and wave number, are linear according to CCM. This yields constant phase velocities. However, experiments showed that for small wavelengths, dispersion curves are nonlinear. Hence, CCM is not capable to represent such material behaviour for small wavelengths. As an alternative approach, peridynamics can be utilised for this purpose. In this study, closed form dispersion relationships are derived and presented according to the original bond-based peridynamics formulation. According to the evaluated results, it can be concluded that peridynamics can capture non-linear frequency-wave number relationship as also observed in real materials.

Keywords: Peridynamics; Dispersion; Wave; Non-local

1. Introduction

Classical continuum mechanics (CCM) has been widely used in structural analysis for the last two centuries. CCM is a local continuum mechanics approach which only takes into account interactions between material points that are directly in contact with each other. The equations of motion of CCM are in the form of partial differential equations. These equations face difficulties if the displacement field is not continuous as a result of a crack since spatial derivatives are not valid along crack surfaces. Moreover, CCM is suitable to represent long-wave propagation

---

* Corresponding author. Tel.: +44-141-548-3876.
  E-mail address: bingquan.wang@strath.ac.uk

behaviour since it doesn't have a length scale parameter. Dispersion curves, which describes the relationship between wave frequency and wave number, are linear according to CCM. This yields constant phase velocities. However, experiments showed that for small wavelengths, dispersion curves are nonlinear. Hence, CCM is not capable to represent such material behaviour for small wavelengths. As an alternative approach, peridynamics can be utilised for this purpose. Peridynamics (PD) (Silling, 2000) is a non-local continuum mechanics formulation whose governing equations are in the form of integro-differential equations. In addition, it has a length scale parameter called horizon which defines the range of non-local interactions between material points. There has been a rapid progress on peridynamics especially during the recent years. The original PD formulation has been extended for multiphysics analysis (De Meo and Oterkus, 2017; Diyaroglu et. al. 2017a,b; Oterkus et. al. 2014; Wang et. al., 2018). PD formulation is also suitable for modelling simplified structures such as beam, plates and shells (Diyaroglu et. al., 2015, 2019; Vazic et. al., 2020; Yang et. al., 2019, 2020). PD can also be applicable for analysis of polycrystalline materials (De Meo et. al., 2016, 2017; Zhu et al., 2016) and nano-structures including graphene (Liu et. al., 2018). PD can also capture complex damage patterns in composite structures (Oterkus et. al., 2010a; Oterkus and Madenci, 2012a,b). PD is suitable for dynamic fracture (Imachi et. al., 2019, 2020; Basoglu et. al., 2019; Vazic et. al., 2017) and impact analysis (Oterkus et. al., 2012). Fatigue analysis can also be performed in peridynamic framework (Oterkus et. al., 2010b). PD was utilized to perform topology optimization of crack structures (Kefal et. al., 2019). An extensive overview of PD research can be found in Madenci and Oterkus (2014) and Javili et. al. (2019).

Dispersion curves have non-linear form in peridynamics so that real material behaviour can be accurately represented for small wavelengths (Bazant, et. al., 2016; Butt, et. al., 2017; Zhang, et. al., 2019). In this study, closed form dispersion relationships are derived and presented according to the original bond-based peridynamics formulation.

2. Peridynamic dispersion relationships

2.1. Peridynamic dispersion relationship for 1-Dimensional models

The equation of motion in bond-based peridynamic theory for the material point x can be written as

$$\rho \ddot{u}(x,t) = \int_V c(x'-x)s(u'-u,x'-x)dV \tag{1}$$

where x, x' are the coordinates of the paired material points, u', u are the displacements of the material points, $c(x'-x)$ is the bond constant, ρ the mass density, $s(u'-u,x'-x)$ is the stretch of the paired material points, which can be expressed in 1-D as

$$s(u'-u,x'-x) = \frac{u'+x'-u-x}{|x'-x|} \tag{2}$$

The equation of motion can be solved with plane wave solution $u(x,t)$

$$u(x,t) = Ue^{i(kx-\omega t)} \tag{3}$$

where U is the constant amplitude vector, k is the wavenumber, ω is the angular frequency in rad/sec. Substituting the plane wave solution given in Eq. (3) in Eq. (1) leads to

$$\rho \omega_{pd}^2 = 2\int_0^\delta \frac{C(\xi)}{\xi}\big(1-\cos(k\xi)\big)Ad\xi \tag{4}$$

where δ is the horizon size, A is the cross-sectional area, and $\xi = |x'-x|$. Bond constant for isotropic materials in a one-dimensional bar can be written as

$$C(\xi) = \frac{2E}{A\delta^2} \tag{5}$$

where E is the elastic modulus. Substituting the bond constant expression given in Eq. (5) in the peridynamic equation of motion with the plane wave solution given in Eq. (4), the analytical solution of the wave dispersion relationship for one-dimensional structures in terms of wave number and the horizon size can be obtained as

$$\omega_{pd}^2 = \frac{4E}{\rho\delta^2}\left(\gamma - \text{cosintegral}(k\delta) + \ln(k\delta)\right) \tag{6}$$

where γ is the Euler gamma constant. Note that dispersion of the peridynamic wave is only related to the micromodulus function, density, and horizon. These parameters are inherent properties of the material.

2.2. Peridynamic dispersion relationships for 2-Dimensional models

The dispersion relationships in two-dimensional models can be obtained similarly. To simplify the calculation, cylindrical coordinate system is utilised. Fig. 1 presents two material points $\mathbf{x}$ and $\mathbf{x}'$ and linked with a bond ξ. u, u', v and v' are displacement components of the material points $\mathbf{x}$ and $\mathbf{x}'$ and represent the longitudinal (x-direction) and transverse (y-direction) displacements, respectively.
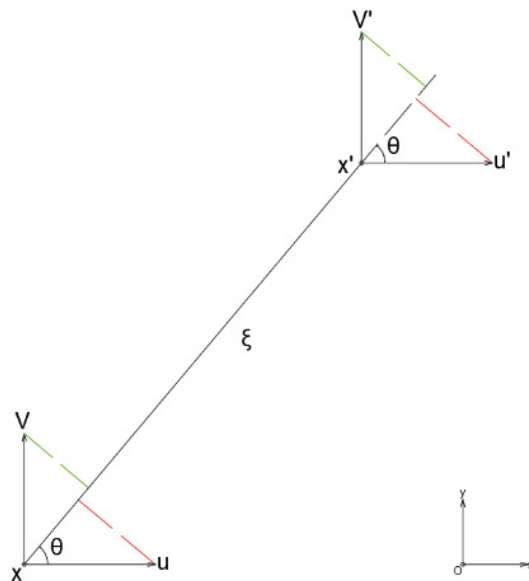

Fig. 1. Displacement components of the material points $\mathbf{x}$ and $\mathbf{x}'$.

As can be observed Fig. 1, the components of the longitudinal and transverse displacements of material points $\mathbf{x}$ and $\mathbf{x}'$ projected on the bond ξ can be written as

$$u_{x\xi} = u\cos\theta \tag{7a}$$
$$u_{y\xi} = v\sin\theta \tag{7b}$$
$$u_{x'\xi} = u'\cos\theta \tag{7c}$$

$$u_{y'\xi} = v' \sin \theta \tag{7d}$$

Hence, the stretch s between two material points becomes

$$s = \frac{(u'-u)\cos\theta + (v'-v)\sin\theta}{\xi} \tag{8}$$

The peridynamic equation of motion with small displacement assumption can be written in longitudinal direction as

$$\rho \ddot{u}(\mathbf{x},t) = \int_V \left(C(\xi) \frac{(u'-u)\cos\theta + (v'-v)\sin\theta}{\xi} \right) \cos\theta \, dV \tag{9}$$

where $C(\xi)$ is the bond constant. Eq. (9) can be rewritten in cylindrical coordinates as

$$\rho \ddot{u}(\mathbf{x},t) = C(\xi) h \int_0^\delta \int_0^{2\pi} \left(\frac{(u'-u)\cos\theta + (v'-v)\sin\theta}{\xi} \right) \cos\theta \, \xi \, d\xi \, d\theta \tag{10}$$

where h is the thickness of the geometry.

While considering the waves propagating in positive x-direction and the transverse displacement of each material point is zero, i.e. $v(\mathbf{x},t) = v(\mathbf{x}',t) = 0$, the equation of motion in the longitudinal direction can be simplified as

$$\rho \ddot{u}(\mathbf{x},t) = C(\xi) h \int_0^\delta \int_0^{2\pi} (u'-u)\cos\theta \cos\theta \, \xi \, d\xi \, d\theta \tag{11}$$

Inserting the plane wave solution

$$u(\mathbf{x},t) = U e^{i(k\mathbf{x}\cdot\mathbf{n}-\omega t)} \tag{12}$$

, where $\mathbf{n}$ is the unit vector describing the direction of the wave propagation, into the equation of motion in the longitudinal direction leads to ($\mathbf{n} = \mathbf{e}_x$)

$$\begin{aligned}
\omega_L^2 \rho &= C(\xi) h \int_0^\delta \int_0^{2\pi} \left(1 - e^{i[k(x'-x)]} \right) \cos^2\theta \, d\xi \, d\theta \\
&= C(\xi) h \int_0^\delta \int_0^{2\pi} \left(1 - e^{i[k\xi\cos\theta]} \right) \cos^2\theta \, d\xi \, d\theta \\
&= C(\xi) h \int_0^\delta \int_0^{2\pi} \left[1 - \cos(k\xi\cos\theta) - i\sin(k\xi\cos\theta) \right] \cos^2\theta \, d\xi \, d\theta \\
&= C(\xi) h \int_0^\delta \int_0^{2\pi} \left[1 - \cos(k\xi\cos\theta) \right] \cos^2\theta \, d\xi \, d\theta
\end{aligned} \tag{13}$$

Please note that $\sin(k\xi\cos\theta)$ is an odd function and its integration leads to zero. Performing the integration in Eq. (13) yields

$$\omega_L^2 \rho = C(\xi) h \pi \left(\delta - \frac{2\text{BesselJ}[1,\delta k]}{k} \right) \tag{14}$$

where $\text{BesselJ}[m,\dots]$ is Bessel function of the m kind. For the two-dimensional structures, $C(\xi)$ is given as

$$C(\xi) = \frac{9E}{\pi h \delta^3} \tag{15}$$

Therefore, the analytical solution of the longitudinal wave dispersion relationship for a two-dimensional structure can be obtained as

$$\omega_L = \sqrt{\frac{9E}{\rho \delta^3}\left(\delta - \frac{2\text{BesselJ}[1,\delta k]}{k}\right)} \tag{16}$$

Similar procedure can be followed for the transverse direction. While considering the waves propagating in positive x-direction and the longitudinal displacement at each material point is zero, i.e. $u(\mathbf{x},t) = u(\mathbf{x}',t) = 0$, yields the equation of motion in transverse direction as

$$\rho \ddot{v}(\mathbf{x},t) = C(\xi)h\int_0^\delta \int_0^{2\pi} (v'-v)\sin\theta \sin\theta \, d\xi d\theta \tag{17}$$

By using the plane wave solution, the equation of motion in the transverse direction results in

$$
\begin{aligned}
\omega_T^2 \rho &= C(\xi)h\int_0^\delta \int_0^{2\pi} \left(1 - e^{i[k(x'-x)]}\right)\sin^2\theta \, d\xi d\theta \\
&= C(\xi)h\int_0^\delta \int_0^{2\pi} \left(1 - e^{i[k\xi\cos\theta]}\right)\sin^2\theta \, d\xi d\theta \\
&= C(\xi)h\int_0^\delta \int_0^{2\pi} \left[1 - \cos(k\xi\cos\theta)\right]\sin^2\theta \, d\xi d\theta
\end{aligned}
\tag{18}
$$

The integration part in Eq. (18) can be solved analytically as

$$
\begin{aligned}
&\int_0^\delta \int_0^{2\pi} \left[1 - \cos(k\xi\cos\theta)\right]\sin^2\theta \, d\xi d\theta = \\
&\pi\left(\delta - \frac{\text{BesselJ}[1,\delta k](-2 + \delta k\pi \, \text{StruveH}[0,\delta k])}{k} + \delta \, \text{BesselJ}[0,\delta k](-2 + \pi \, \text{StruveH}[1,\delta k])\right)
\end{aligned}
\tag{19}
$$

where $\text{StruveH}[m,\dots]$ is Struve function of the m kind. Therefore, by using the bond constant expression for a two-dimensional structure given in Eq. (15), the analytical solution of the transverse wave dispersion relationship can be obtained as

$$\omega_T = \sqrt{\frac{9E}{\rho \delta^3}\left(\delta - \frac{\text{BesselJ}[1,\delta k](-2 + \delta k\pi \, \text{StruveH}[0,\delta k])}{k} + \delta \, \text{BesselJ}[0,\delta k](-2 + \pi \, \text{StruveH}[1,\delta k])\right)} \tag{20}$$

2.3. Peridynamic dispersion for 3-Dimensional models

To derive the wave dispersion relationships for three dimensional structures, spherical coordinates can be utilised as shown in Fig. 2.
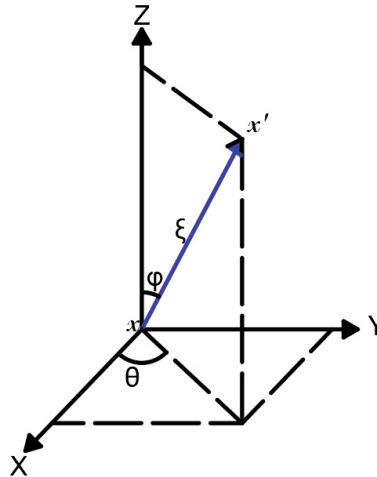

Fig. 2. Spherical coordinate system.

where ξ indicates the bond distance between two material points, θ is the angle around the z-axis, φ is the angle between the radial line and the z-axis. By following a similar procedure as in 2-Dimensional structures, the wave dispersion relationships, ω_L : longitudinal (*x*-) direction, ω_T : transverse (*y*-) direction, ω_V : vertical (*z*-) direction can be obtained as

$$\omega_L = \sqrt{\frac{12E}{\rho\pi\delta^4} \int_0^{2\pi} \frac{2 - \pi\,\text{StruveH}[-1,\delta k\cos\theta] - \pi\,\text{StruveH}[1,\delta k\cos\theta] + \delta k\pi\cos\theta\,\text{StruveH}[2,\delta k\cos\theta]}{k^2} d\theta} \qquad (21a)$$

$$\omega_T = \sqrt{\frac{12E}{\rho\pi\delta^4} \int_0^{\pi/2} \frac{4\left(2 - \pi\,\text{StruveH}[-1,\delta k\cos\theta] - \pi\,\text{StruveH}[1,\delta k\cos\theta] + \delta k\cos\theta\,\text{StruveH}[2,\delta k\cos\theta]\right)\text{Tan}^2\theta}{k^2} d\theta}$$

$$(21b)$$

$$\omega_V = \sqrt{\frac{12E}{\rho\pi\delta^4} \int_0^{\pi}\int_0^{\pi} \cos^2\varphi \left[\frac{\delta^2\sin\varphi - \csc\dfrac{\varphi}{2}\sec\theta\sec\dfrac{\varphi}{2}\left(\left[-1+\cos\left(\delta k\cos\theta\sin\varphi\right)\right]\sec\theta + \delta k\sin\varphi\sin\left[\delta k\cos\theta\sin\varphi\right]\right)}{k^2} \right] d\varphi\, d\theta}$$

$$(21c)$$

3. Numerical results

In this section, dispersion relationships obtained in the previous section are visually presented for the copper material for both 1-D, 2-D and 3-Dimensional structures. Copper has a density of 8960 kg/m³, Young's modulus of 130 GPa, and Poisson's ratio of 0.34. Lattice constant of copper is 3.598 A. The horizon size is specified as $\delta = 3\times10^{-10}$ m . The wave number in dispersion curves is normalized by dividing the wave number with $2\pi / a$ where a is the lattice constant.
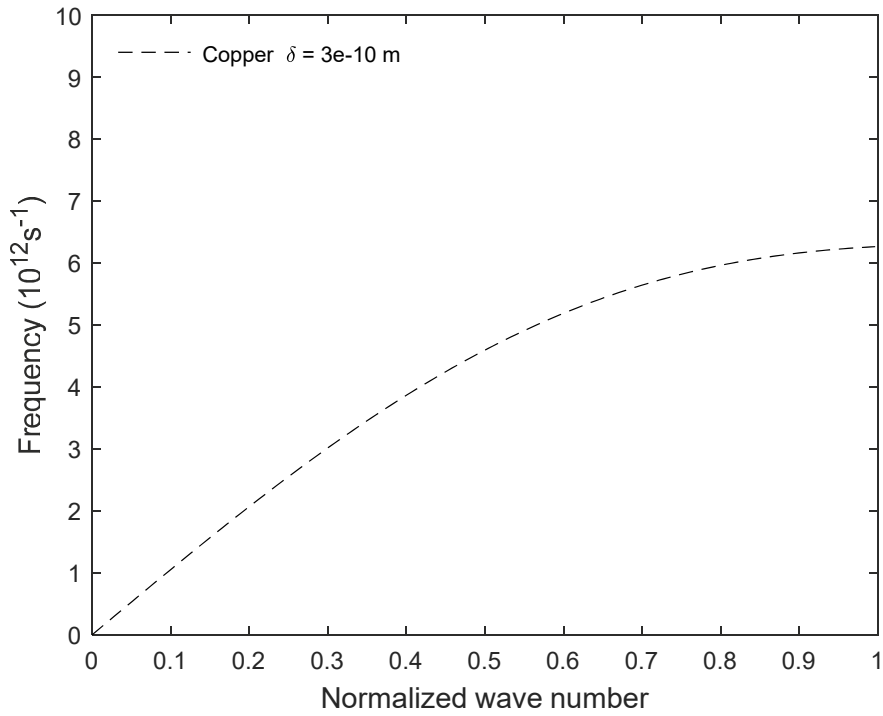
Fig. 3. Dispersion relationship for a 1-Dimensional structure made of copper.
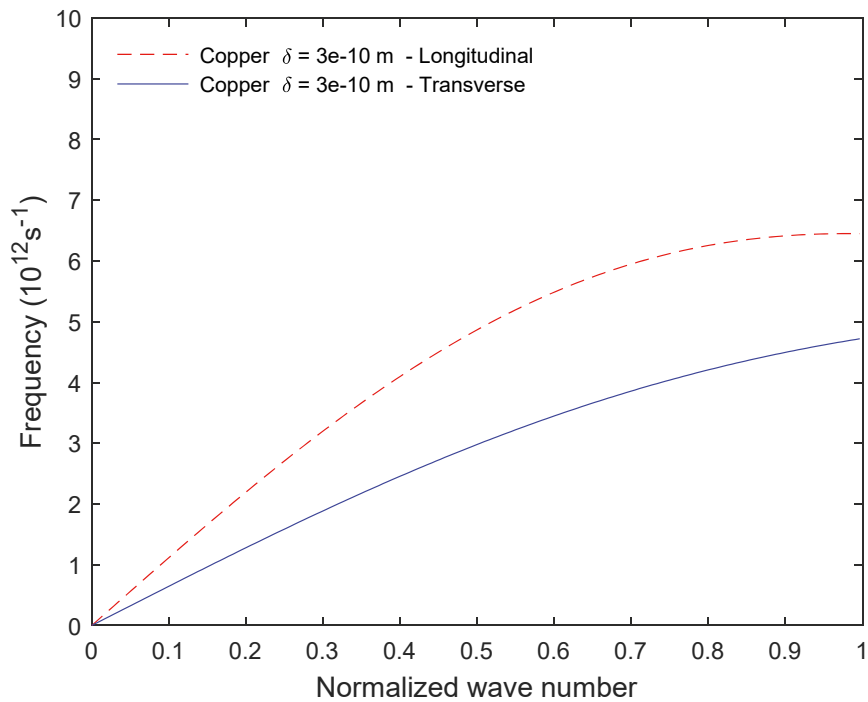

Fig. 4. Dispersion relationship for a 2-Dimensional structure made of copper.
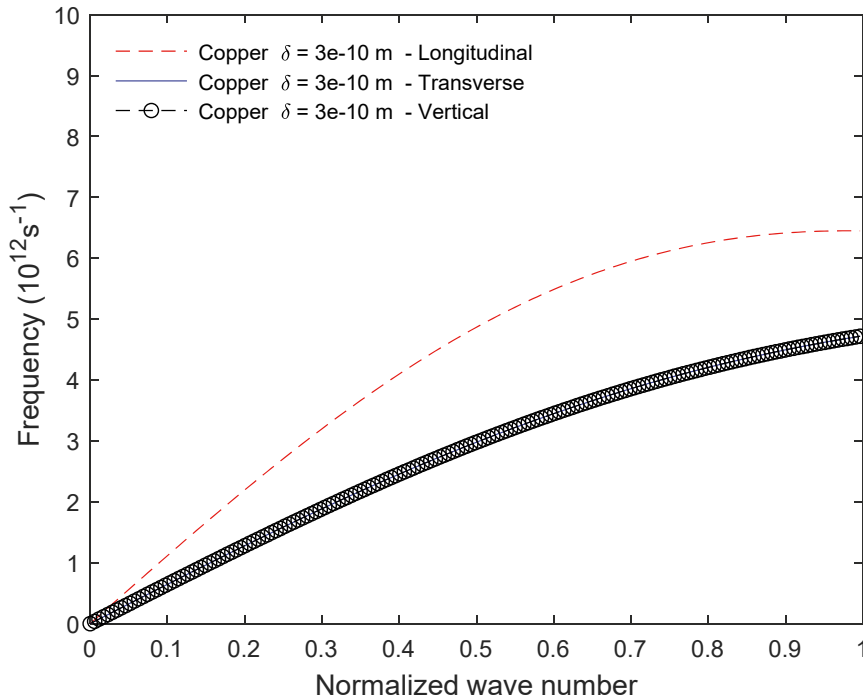
Fig. 5. Dispersion relationship for a 3-Dimensional structure made of copper.

Dispersion relationships for 1-D, 2-D and 3-Dimensional structures made of copper are depicted in Figs. 3-5. As shown in these figures, peridynamics captures non-linear frequency-wave number relationship as also observed in real materials.

4. Conclusions

In this study, closed form dispersion relationships were derived and presented according to the original bond-based peridynamics formulation. Peridynamic dispersion relationships were visually shown for the copper material for both 1-D, 2-D and 3-Dimensional structures. According to the results, it was concluded that peridynamics can capture non-linear frequency-wave number relationship as also observed in real materials.

Acknowledgements

References

Basoglu, M.F., Zerin, Z., Kefal, A., Oterkus, E., 2019. A computational model of peridynamic theory for deflecting behavior of crack propagation with micro-cracks. Computational Materials Science 162, 33–46.
Bažant, Z.P., Luo, W., Chau, V.T., Bessa, M.A., 2016. Wave dispersion and basic concepts of peridynamics compared to classical nonlocal damage models. Journal of Applied Mechanics 83(11).
Butt, S.N., Timothy, J.J., Meschke, G., 2017. Wave dispersion and propagation in state-based peridynamics. Computational Mechanics 60(5), 725–738.
De Meo, D., Zhu, N., Oterkus, E., 2016. Peridynamic modeling of granular fracture in polycrystalline materials. Journal of Engineering Materials and Technology 138(4), 041008.
De Meo, D., Oterkus, E., 2017. Finite element implementation of a peridynamic pitting corrosion damage model. Ocean Engineering 135, 76–83.
De Meo, D., Russo, L., Oterkus, E., 2017. Modeling of the onset, propagation, and interaction of multiple cracks generated from corrosion pits by using peridynamics. Journal of Engineering Materials and Technology 139(4), 041001.

Diyaroglu, C., Oterkus, E., Oterkus, S., Madenci, E., 2015. Peridynamics for bending of beams and plates with transverse shear deformation. International Journal of Solids and Structures, 69, 152–168.

Diyaroglu, C., Oterkus, S., Oterkus, E., Madenci, E., 2017a. Peridynamic modeling of diffusion by using finite-element analysis. IEEE Transactions on Components, Packaging and Manufacturing Technology 7(11), 1823–1831.

Diyaroglu, C., Oterkus, S., Oterkus, E., Madenci, E., Han, S., Hwang, Y., 2017b. Peridynamic wetness approach for moisture concentration analysis in electronic packages. Microelectronics Reliability 70, 103–111.

Diyaroglu, C., Oterkus, E., Oterkus, S., 2019. An Euler–Bernoulli beam formulation in an ordinary state-based peridynamic framework. Mathematics and Mechanics of Solids 24(2), 361–376.

Imachi, M., Tanaka, S., Bui, T.Q., Oterkus, S., Oterkus, E., 2019. A computational approach based on ordinary state-based peridynamics with new transition bond for dynamic fracture analysis. Engineering Fracture Mechanics 206, 359–374.

Imachi, M., Tanaka, S., Ozdemir, M., Bui, T.Q., Oterkus, S., Oterkus, E., 2020. Dynamic crack arrest analysis by ordinary state-based peridynamics. International Journal of Fracture 221(2), pp.155–169.

Javili, A., Morasata, R., Oterkus, E., Oterkus, S., 2019. Peridynamics review. Mathematics and Mechanics of Solids 24(11), 3714-3739.

Kefal, A., Sohouli, A., Oterkus, E., Yildiz, M., Suleman, A., 2019. Topology optimization of cracked structures using peridynamics. Continuum Mechanics and Thermodynamics 31(6), 1645–1672.

Liu, X., He, X., Wang, J., Sun, L., Oterkus, E., 2018. An ordinary state-based peridynamic model for the fracture of zigzag graphene sheets. Proceedings of the Royal Society A: Mathematical, Physical and Engineering Sciences 474(2217), p.20180019.

Madenci, E., Oterkus, E., 2014. Peridynamic theory. Springer, New York, NY.

Oterkus, E., Barut, A., Madenci, E., 2010a. Damage growth prediction from loaded composite fastener holes by using peridynamic theory. In 51st AIAA/ASME/ASCE/AHS/ASC Structures, Structural Dynamics, and Materials Conference 18th AIAA/ASME/AHS Adaptive Structures Conference, Orlando, Florida, USA, p. 3026.

Oterkus, E., Guven, I. and Madenci, E., 2010b. Fatigue failure model with peridynamic theory. In 12th IEEE Intersociety Conference on Thermal and Thermomechanical Phenomena in Electronic Systems, Las Vegas, Nevada, USA, p. 1-6.

Oterkus, E., Madenci, E., 2012a. Peridynamics for failure prediction in composites. In 53rd AIAA/ASME/ASCE/AHS/ASC Structures, Structural Dynamics and Materials Conference 20th AIAA/ASME/AHS Adaptive Structures Conference, Honolulu, Hawaii, USA, p. 1692.

Oterkus, E., Madenci, E., 2012b. Peridynamic theory for damage initiation and growth in composite laminate. Key Engineering Materials 488, 355–358.

Oterkus, E., Guven, I., Madenci, E., 2012. Impact damage assessment by using peridynamic theory. Open Engineering 2(4), 523–531.

Oterkus, S., Madenci, E., Oterkus, E., Hwang, Y., Bae, J., Han, S., 2014, May. Hygro-thermo-mechanical analysis and failure prediction in electronic packages by using peridynamics. In 2014 IEEE 64th Electronic Components and Technology Conference (ECTC), Orlando, Florida, USA, p. 973-982.

Silling, S.A., 2000. Reformulation of elasticity theory for discontinuities and long-range forces. Journal of the Mechanics and Physics of Solids 48(1), 175–209.

Vazic, B., Wang, H., Diyaroglu, C., Oterkus, S., Oterkus, E., 2017. Dynamic propagation of a macrocrack interacting with parallel small cracks. AIMS Materials Science 4(1), pp.118–136.

Vazic, B., Oterkus, E., Oterkus, S., 2020. Peridynamic model for a Mindlin plate resting on a Winkler elastic foundation. Journal of Peridynamics and Nonlocal Modeling, pp.1–10.

Wang, H., Oterkus, E., Oterkus, S., 2018. Predicting fracture evolution during lithiation process using peridynamics. Engineering Fracture Mechanics 192, 176–191.

Yang, Z., Oterkus, E., Nguyen, C.T., Oterkus, S., 2019. Implementation of peridynamic beam and plate formulations in finite element framework. Continuum Mechanics and Thermodynamics 31(1), 301–315.

Yang, Z., Vazic, B., Diyaroglu, C., Oterkus, E., Oterkus, S., 2020. A Kirchhoff plate formulation in a state-based peridynamic framework. Mathematics and Mechanics of Solids 25(3), 727–738.

Zhang, X., Xu, Z., Yang, Q., 2019. Wave dispersion and propagation in linear peridynamic media. Shock and Vibration 2019, 9528978.

Zhu, N., De Meo, D., Oterkus, E., 2016. Modelling of granular fracture in polycrystalline materials using ordinary state-based peridynamics. Materials 9(12), p.977.